Bio-sorption for Effective Removal of Chromium (VI) from Wastewater Using *Moringa Stenopetala* Seed Powder (MSSP) and Banana Peel Powder (BPP)

Tolera Seda Badessa*, Esayas Wakuma, Ali Mohammed Yimer
Department of Chemistry, College of Natural Sciences, Arba Minch University, Ethiopia
Corresponding Author's Email: toleraseda@yahoo.com

Abstract: *Chromium is an extremely toxic metal in the form of Cr (VI) that causes severe environmental and health problems. Therefore, the aim of this study was to remove chromium ions from wastewater by using cost effective and environmentally friendly bio-sorbents; Moringa stenopetala Seed Powder (MSSP), and Banana Peel Powder (BPP) and to evaluate its adsorption capacities as bio-sorbents.* FT-IR characterization of the adsorbents showed that there was a change in the functional groups of the structure of both adsorbents before and after the adsorption that might be due to the adsorption processes taken place on the surface of adsorbent. *Adsorption experiments were carried out as batch studies with different contact times, pH, adsorbent dose, initial metal ion concentration, and temperature. Results showed maximum removal efficiency for Cr (VI) at 120 minutes contact time, adsorbent dose of 20 g/L and pH 2 by MSSP and pH 4 by BPP. The percentage removal of Cr(VI) increased with increasing adsorbent dose(from 5g/L to 20 g/L) and contact time (from 60 min to 120 min). Freundlich isotherm model showed a better fit to the equilibrium data than the Langmuir model. The kinetics of adsorption for chromium was well represented by pseudo-second order kinetic model and the calculated equilibrium sorption capacity of the model showed good agreement with the sorption capacity obtained from Experimental results.*

Keywords: *Moringa stenopetala*, Banana peel, Chromium (VI), FT-IR, Adsorption Isotherms

1. Introduction

Chromium is a naturally occurring metal found in the environment commonly in trivalent, Cr(III), and hexavalent, Cr(VI) forms [1, 2]. The trivalent state of chromium (Cr(III)) is essential for carbohydrate metabolism in humans, whereas hexavalent chromium (Cr(VI)) is considered to be toxic [3, 4]. The hexavalent chromium is a hundred-fold more toxic than trivalent form of chromium [5, 6]. This is due to the fact that it is a strong oxidizing agent that can release free radicals that can have carcinogenic effects on cells [4]. Chromium containing compounds in the form of hexavalent is used widely in different industries such as leather industry, electroplating, textile dyeing, and metal fabrication and finishing [7]. Chromium containing wastewater is one of the major pollutants of the environment. Hence, industries must treat the effluents to reduce the Chromium ions concentration in water and wastewater to acceptable levels before releasing it into the natural environment. Various conventional and advanced treatment methods have been employed for the removal of Cr ions from water and wastewater in developed countries. These include chemical precipitation, ion exchange, reverse osmosis, membrane filtration, electrodialysis, polymeric nano particles and activated carbon adsorptions [8-13]. However, these conventional and advanced technologies are expensive and non-regenerable materials used, generation of toxic sludge is often ineffective, particularly for the removal of Cr ions at low concentrations and also difficult to apply them in developing countries like Ethiopia [14-16].

Moringa is a tropical plant belonging to the family of moringaceae that grows throughout the tropical regions. Moringa oleifera and moringa stenopetala are the two most common species among the various species of the moringa family [17, 18]. Moringa stenopetala is domesticated in the east African low lands and is indigenous to southern Ethiopia. Moringa stenopetala is often called “cabbage tree” and is an important indigenous vegetable in south Ethiopia where it is cultivated as a food crop. [19, 20]. The water soluble moringa seed possess coagulating properties similar to those of synthetic cationic polymers. Moringa seeds contain cationic polypeptides with various functional groups, particularly low molecular weight amino acids. These amino acids are de-protonated to carboxylate ligands at pH range of 4 to 8 simultaneously protonating the amino group which facilitates the binding of positively charged ions with the carboxylic group [21, 22]. The use of bio-adsorbents like moringa stenopetala seed powder that are easily available and effective for removal of metals could be an innovative and economical approach for treatment of industrial wastewater.

Banana is another plant most widely grown in tropical regions, cultivated over 130 countries. Ethiopia, which lies entirely in the tropics, has great potential for banana production [23]. Cavendish banana is the major fruit crop that widely grown and consumed in Ethiopia especially in the south and south western part of the country [24]. Banana is rich in polyphenols, flavonoids and dopamine which exist both in the pulp and the peel [25]. The pectin substances are complex hetero polysaccharides containing galacturonic acid, arabinose, galactose, and rhamnose as the major sugar constituents; the carboxyl groups of galacturonic acid allow pectin substances to strongly bind metal cations in aqueous solution [26]. Thus, banana peels powder could be used for the bio-adsorption of metal ions in wastewaters. The needs for cost-effective, eco-friendly and locally available alternative materials for the removal of chromium ion from aqueous solutions is essential. Therefore, *Moringa Stenopetala* Seed Powder *a*nd Banana peel powder for their adsorptive removal of Cr(VI) ions from aqueous solutions under various operating variables (contact time, solution pH, initial Cr concentration and temperature) was the focus of the current work.

2. Materials and Methods

2.1 Preparation of *Moringa Stenopetala* Seed Powders (MSSP)

Matured and fresh seeds of *Moringa stenopetala* were collected from Arba Minch University and specimen identification of the seed was done at Addis Ababa University National Herbarium. Then the seeds were separated from their cover or shell manually. They were, air-dried and ground using a grinding mill and sieved through a mesh. Finally, the fine powder of the seed shown in Fig. 2.1 B, was collected and kept in a clean bottle until experiments were done.

Figure 2.1Moringa Stenopetala Sample A/ Seed and B/ Seed powder

2.2 Preparation of banana peel Powders (BPP)

The banana fruits were collected from the local market of Arba Minch City, and the peel shown in Fig. 2.2 was separated from the fruits and cut into smaller pieces while washing thoroughly

with tap and distilled water to remove dirt particles. Finally, the wetted banana peel was air-dried, ground into a powder, and kept in a clean airtight bottle; until experiments were done.

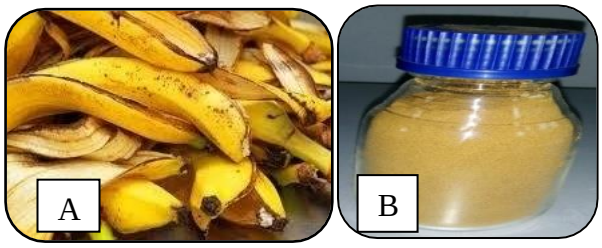

Figure 2.2 Banana peel Sample A/ Raw Peel B/ Peel powder

2.3 Preparation of Adsorbate

A 1000 mg/L of Cr(VI) stock solution was prepared (2.827 g of $K_2Cr_2O_7$ in 1000 mL volumetric flask using distilled-deionized water) [27]. Then a series of working standard solutions of different concentrations were prepared by appropriate dilution of the stock solution.

2.4 Batch Experiments

All experiments were carried out in batch mode to obtain both the thermodynamic and kinetic information. The studies were carried out at the optimized contact time, pH value, and adsorbent dosage. Before adding the adsorbent, the pH of the solution was adjusted by using 0.1 M NaOH or 0.1 M HCl solutions. To ensure equal mixing of the solution, all the experiments were performed with an orbital shaker with a constant agitation speed of 150 rpm. The equilibrium study was conducted and compared with Langmuir and Freundlich isotherm models. The kinetics experiments were studied using pseudo-first-order and pseudo-second-order models. After completing the batch experiment, the solution was separated from the adsorbent and digested in a microwave digester for the determination of its concentration using GFAAS. The blank solutions that contain the adsorbents before adsorption were also digested in the same way that the samples were done, and analysed for the chromium content The method detection limit was developed from the results to control the interferences coming from the adsorbent nature. Therefore, the result of adsorbed chromium was reported based on the method detection limit. Then, the adsorption efficiency (%) and capacity at a given contact time for the selected adsorbents were determined using equations 1and 2 [28, 29].

$$\% \text{ Removal} = \frac{(C_0 - Cf)}{C_0} \text{ x } 100 \quad (1)$$

$$q = \frac{(C_0 - C_f)\mathrm{V}}{m} \quad (2)$$

where C_0 = initial concentration, Cf = concentration after adsorption, q = metal removal in mg/g, m = adsorbent mass in gram and V = volume of wastewater used during the experiment.

2.5 Adsorption Isotherm

The adsorption isotherm is a graphical representation of expressing the amount of solute adsorbed per unit mass of adsorbent as a function of equilibrium concentration in bulk solution at constant temperature. The experiments were carried out under different adsorbent dose that ranged from 0.5 – 2 g with an interval of 0.5 g by keeping the previously determined parameters at the optimal level in 100 mL solution of the metal ion with an agitation speed of 150 rpm. Then, the experiments were designed and conducted for the evaluation of adsorption equilibria between the adsorbate and adsorbent and finally compared with the existing models. The results were found to be fitting both the Langmuir and Freundlich adsorption isotherm models [30-33].

The Langmuir model assumes that uptake of adsorbate molecule occurs on a homogenous surface by monolayer adsorption without any interaction between adsorbed molecules and uniform energies of adsorption [34]. The Langmuir equation is represented as

$$q_e = \frac{(q_m \, \mathrm{b} C_e)}{(1 + \mathrm{b} C_e)} \tag{3}$$

where C_e is the equilibrium concentration of the ion (mg/L); q_e is the amount of ion adsorbed (mg/g); q_m is q_e for a complete monolayer (mg/g); and b is the bio-sorption equilibrium constant (L/mg).

The linear form of Langmuir isotherm model can be represented by using equation (4):

$$\frac{C_e}{q_e} = \left(\frac{1}{q_m \mathrm{b}}\right) + \left(\frac{C_e}{q_m}\right) \tag{4}$$

The essential characteristics of the Langmuir isotherm can be explained by the equilibrium separation factor R_L, defined as:

$$R_L = \frac{1}{(1 + \mathrm{b} C_o)} \tag{5}$$

where b is the Langmuir constant and C_o is the highest metal concentration (mg/L).

Depending on the value of R_L, the shape of the isotherm and whether the bio-sorption is favourable or not, can be determined. The types of isotherms with R_L values are given in [35 – 37].

Freundlich isotherm model describes a multi-layer bio-sorption based on adsorption on heterogeneous surface and adsorption capacity which is related to the concentration of the adsorbent. The model can be presented as [38]

$$q_e = K_f C_e^{1/n} \quad (6)$$

where q_e is the amount of ion adsorbed (mg/g); C_e is the equilibrium concentration (mg/L); K_f and 1/n are empirical constants, indicating the adsorption capacity (Freundlich constant) and adsorption intensity (which varies with the heterogeneity of the material)., respectively.

The two Freundlich parameters K_f and 1/n can be determined graphically by plotting the experimental data and then using the Freundlich equation in the following form

$$\ln q_e = \ln K_f + {}^{1}/_{n} \ln C_e \quad (7)$$

where K_f and 1/n are evaluated from the intercept and slope of the plot of $\ln q_e$ vs $\ln C_e$. For values in the range $0.1<1/n<1$, bio-sorption is favourable. The greater the values of K_f, better is the favourability of bio-sorption.

2.6 Adsorption Kinetics

The effect of time on the removal rate of Cr(VI) ion from the solution were investigated using kinetic study. Adsorption kinetics shows a large dependence on the physical and/or chemical characteristics of the adsorbent material. The experiment was conducted in a separate 250 mL Erlenmeyer flask by keeping pH, adsorbent dose and metal ion concentration at the optimum level in different time intervals (30 min., 60 min., 90 min., 120 min. and 150 min.) by adjusting the agitation speed at 150 rpm. Finally, the experimental data were analyzed using pseudo first-order [32] and pseudo-second order [33] kinetics models.

Pseudo-first order kinetics model was based on adsorption capacity of adsorbent and suggests that there are no interactions between ions and each ion sorbs on a local site. Therefore, the designed experiment for the bio-sorption process was undergone the pseudo-first order kinetics as the adsorption is occurring as monolayer on the surface of adsorbent and the equation is expressed as [32]:

$$\frac{dq_t}{dt} = k_1 (q_e - q_t) \quad (8)$$

Where q_e and q_t are the amounts (mg/g) of adsorbed pollutant on the adsorbent at equilibrium and time t; and k_1 is the rate constant (min^{-1}) of Lagergren's first-order adsorption.

After integration and applying boundary conditions t=0 to t=t and q_t=0 to q_t=q_e, the integrated form becomes:

$$\log(q_e - q_t) = \log q_e - \frac{k1t}{2.303} \quad (9)$$

The plot of log (q_e- q_t) versus t gives a straight line for first-order adsorption kinetics which allows the computation of the rate constant k_1 and q_e from the slop and intercept of the plot.

The pseudo-second-order kinetics model is based on the assumption that the bio-sorption follows a second order mechanism and the occupation rate of the adsorption site is proportional to the square of the number of unoccupied sites. The rate equation can be represented in the following form [33].

$$\frac{dq_t}{dt} = k_2(q_e\text{-}q_t)^2 \quad (10)$$

where k_2 is the rate constant (g/mg min) of second-order adsorption.

The integrated form of the equation (10) becomes:

$$\frac{1}{q_e - q_t} = \frac{1}{q_e} + k_2 t \quad (11)$$

The linear form of equation (11) is as follows:

$$\frac{t}{q_t} = \frac{1}{k_2 q_e 2} + \frac{1}{(q_e)\,\mathrm{t}} \quad (12)$$

The k_2 and q_e values of the pseudo-second-order kinetic model can be determined from the intercept and slope of the plots of t/q_t versus t.

2.7 Thermodynamic Study

Thermodynamic parameters provide in-depth information of inherent energetic changes that are associated with adsorption. The thermodynamic parameters such as standard Gibbs free energy change ΔG^o, standard enthalpy change ΔH^o, and standard entropy change ΔS^o gives a better understanding of the effect of temperature on adsorption. These parameters were determined using the following equations [39].

$$\Delta G^o = -RT\, ln\, K_c \quad (13)$$

$$K_c = \frac{C_a}{C_e} \quad (14)$$

The Gibbs free energy change (ΔG^0) is related to the entropy change (ΔS^0) and enthalpy change (ΔH^0) at constant temperature using equation 15:

$$\Delta G^0 = \Delta H^0 - T\Delta S^0 \quad (15)$$

By combining the above two equations we get the following equation:

$$\ln K_c = \frac{\Delta S^0}{R} - \frac{\Delta H}{RT} \quad (16)$$

where K_c is the equilibrium constant, T is the absolute temperature (K), R is the universal gas constant (8.314 J mol^{-1} K^{-1}), C_a (mg/L) is the amount of metal ion adsorbed at equilibrium, C_e (mg/g) is the amount of metal ion left in the solution at equilibrium. The values of ΔH^0 and

ΔS^0 were calculated from the slope and intercept of the Van't Hoff plot of $\ln K_c$ versus 1/T equation (27).

3. Results and Discussion

3.1.FT-IR result for BPP and MSSP

The FT-IR spectra before and after adsorption of chromium were given for both BPP and MSSP in which the absorption peaks appeared in the wavenumber range of 3500cm-^{1}to 625 cm^{-1}. The Fig, 3.1a shows the absorbance spectra of BPP and MSSP before adsorption and Fig.3.1b indicates the absorbance spectra of BPP and MSSP after adsorption of chromium taken place. The spectra containing weak bands in both figures represent the absorbance spectra of BPP before and after adsorption where as the one containing stronger bands in both figures are indicating the absorbance spectra of MSSP before and after adsorption

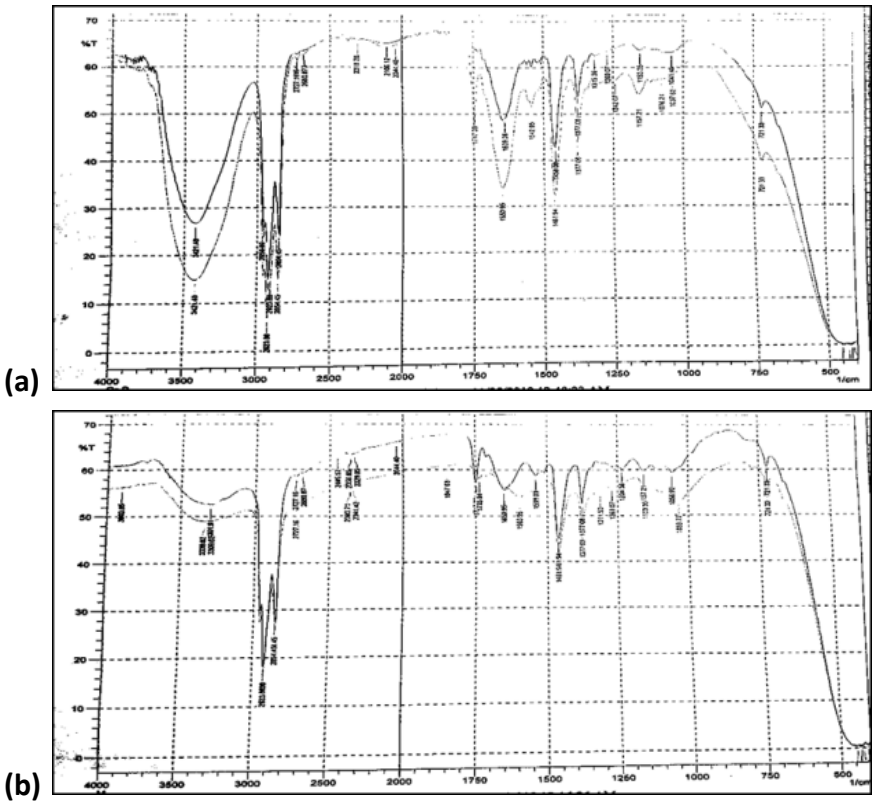

Figure 3.1 FT-IR Spectra of a) BPP and MSSP Before adsorption b) BPP and MSSP after adsorption

The FT-IR spectra in Fig. 3.1a show that broad bands at 3337 cm^{-1}and 3310 cm^{-1} indicate that O-H stretching vibration of carboxylic acid for both BPP and MSSP. These bands disappeared (decreased highly in intensity) in Fig. 3.1b, which confirms that the adsorption of chromium by both adsorbents was highly effective. In the same way a band at 1654cm^{-1} in both figures

indicate that stretching vibration of C=O group in carboxylic acid. In Fig. 3.1b these bands for both BPP and MSSP were also decreased in intensity that confirms adsorption of chromium on both adsorbents.

3.2 Effect of Contact Time

The percentage removal of Cr(VI) ions and the adsorption capacity of MSSP and BPP as a function of contact time was conducted at 60, 90, 120 and 150 minutes using different pH and dose at a constant initial concentration, agitation speed and temperature. The experimental results shown in Fig.3.2 indicate that the percentage removal of Cr(VI) ion increases with increasing contact time up to 120 minutes. Further increase in contact time did not make any change in removal and adsorption capacity. Higher removal efficiency and adsorption capacity was observed at 120 minutes for both the adsorbents. Hence, 120 min was chosen as the equilibrium time. Because at the beginning of the process, adsorption is fast due to the availability of large active binding site but as time has gone, the process slow down as active binding sites are filled by the metal ion.

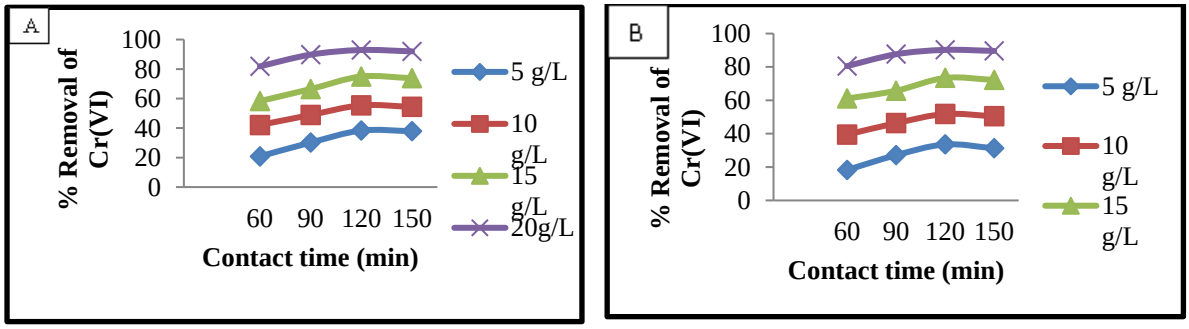

Figure 3.2. Effect of contact time on % removal of: A/ Cr(VI) by MSSP and B/ Cr(VI) by BPP (concentration 30mg/L, contact time 60, 90, 120 &150 minutes, adsorbent dose 5, 10, 15 & 20 g/L solution, agitation speed 150 rpm and pH = 2 for MSSP, pH = 4 for BPP)

3.3 Effect of pH

Solution pH is one of the most important parameters while assessing the adsorption capacity of an adsorbent for metal ion sequestration from aqueous. The pH of the system controls the adsorption capacity due to its influence on the surface properties of the adsorbent and ionic forms of the chromium solutions.

Cr(VI) adsorption was studied as a function of pH over a range of 2 - 8 for MSSP and BPP at an initial concentration of 30 mg/L wastewater. The results of the experiment shown in Figure 3 indicate that optimal Cr(VI) removal efficiency of MSSP and BPP were obtained at pH 2.0 and pH4.0 respectively for120 min contact time. It is evident that chromium (VI) removal efficiency increases with decrease in pH [31]. The favorable effect at low pH might be due to the neutralization of negative changes on the surface of the adsorbents by excess hydrogen ions, thereby facilitating the diffusion of the hydrogen chromate ion ($HCrO_4^-$) and its subsequent adsorption, because $HCrO_4^-$ is the dominant anionic form of Cr(VI) between pH 1.0 and 4.0. This ionic form was found to be preferentially adsorbed on the surface of the adsorbent. The possible explanation for higher adsorption in the acidic region is that the $Cr_2O_7^{2-}$ ion is oxidized to Cr_3^+. Being small in size, it can be easily replaced by the positively charged species The following reaction mechanism might be taken place during adsorption processes on the surface of adsorbents [40, 41].

$$2H + +2HCrO_4^- \leftrightarrow 2H_2CrO_4 \leftrightarrow \ 2H_2O + Cr_2O_7^{2-} + 2H^+$$

$$2H_2O + Cr_2O_7^{2-} + 2H^+ \leftrightarrow 2H_2Cr_4 \leftrightarrow 2CrO_3 + 2H_2O$$

Therefore, Chromium removal in mg/g by MSSP and BPP increases with increasing contact time from 60-120 min. for all pH values; this is because the solution pH is directly related to the large availability of positively charged active sites on the surface of the adsorbent to bind with the metal ions as the solution pH decreases, the surface of the adsorbents exhibits increasing positively charged active sites. As pH decreases, the removal efficiency becomes increasing that was shown in Fig. 3.3. The maximum adsorption of Cr(VI) was observed at the acidic range because, at lower pH, there is an increase in H^+ ions on the adsorbent surface, and the presence of $HCrO_4^-$ ions result in significantly strong electrostatic attraction [42].

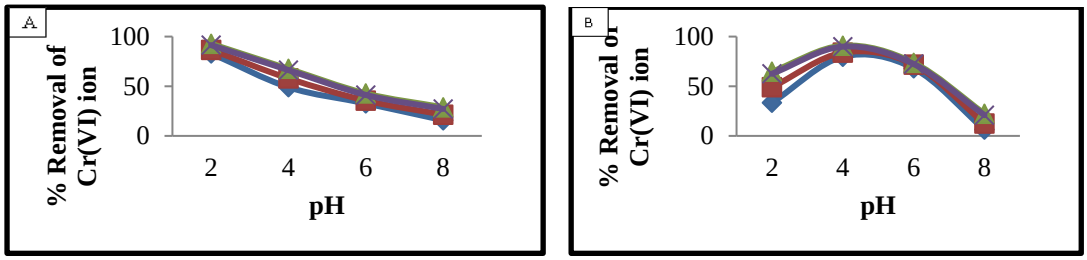

Figure 3.3. Effect of solution pH on % removal of: a/ Cr(VI) by MSSP and b/ Cr(VI) by BPP (concentration 30mg/L, pH, 2, 4, 6 & 8 and contact time 60, 90, 120 & 150 minutes, agitation speed 150 rpm)

3.4 Effect of Adsorbent Dose

The effect of the adsorbent dose on the removal of Cr(VI) ions onto MSSP and BPP was conducted by using 5, 10, 15 and 20 g/L of adsorbent dose under variable pH and contact time on keeping agitation speed and initial concentration constant. Fig.3.4 shows that the percent removal of chromium by MSSP increases from 24.85% to 90.96% and by using BPP it ranges from 20.06% to 89.62% with an increase in adsorbent dose from 5 to 20 g/L at all pH values. The increase in adsorbent dose generally increases the percent removal of the metal ion due to increased surface area of the adsorbent which increases the number of available binding sites for the adsorption process. On the other hand, the quantity of adsorbate metal ion per unit weight of the adsorbent decreases with increasing in the adsorbent dose and this may be due to high adsorbent concentration. If the available metal ion to be sorbed is not sufficient to completely cover the available active sites of the adsorbents, it is leading to the reduction of metal ion uptake [43].

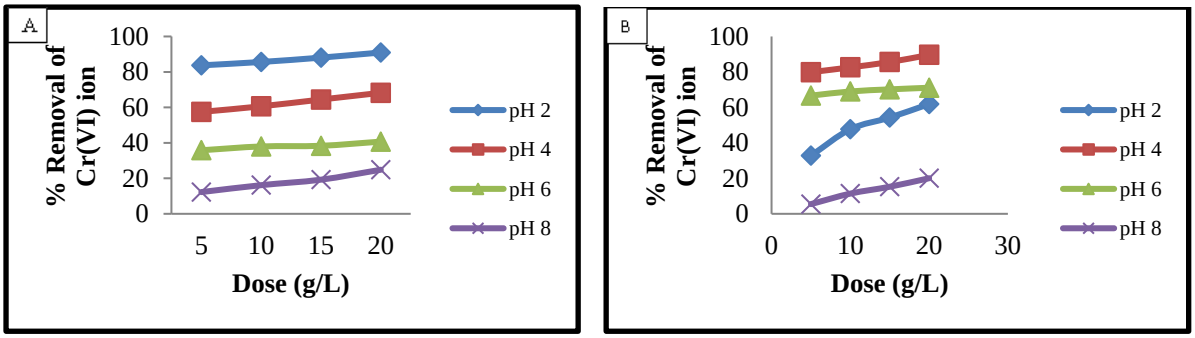

Figure 3.4.Effect of adsorbent dose on % .removal of: a/ Cr(VI) by MSSP and b/ Cr(VI) by BPP (concentration 30 mg/L, agitation speed rpm, *adsorbent dose 5, 10, 15 and 20 g/L solution, pH 2, 4, 6 & 8).*

On the other hand, adsorption capacity in mg/g decreases with increasing adsorbent dose for all pH values. The highest removal efficiency was observed at 5 g/L of adsorbent. Adsorbent dose has also its own effect on the removal efficiency at various contact time. Higher adsorption was obtained at 20 g/L for all contact times but at this dose percent removal variations among different contact times were small. This may be explained by the presence of screening effect when the adsorbent dose increases [44]. Thus, the removal efficiencies of chromium ions at optimal adsorbent concentration were selected as 20 g/L [45].

3.5 Effect of Initial Concentration of chromium

The experiment was carried out under optimal conditions and different initial concentration ranging from 30 mg/L up to 60 mg/L with an interval of 10 mg/L. As shown in Fig.3.5, the increasing of the initial concentration of chromium increases adsorption capacity of the adsorbents but decreases percentage removal of the metal. Maximum % removal of chromium by MSSP is 92.17% and by BPP is 90.07 at 30 mg/L. The decrease in percentage removal of the metal ion with increasing initial concentration may be due to the saturation of adsorption sites on the adsorbent surface. This can be explained by the fact that, at low concentration, the metal ions interact with the binding sites and result in maximum adsorption. This is because, at low concentration, the ratio of available surface to the initial metal ion concentration is larger, so the removal is higher [47]. On the other hand, maximum Cr(VI) ion adsorption capacity of MSSP is 1.71 mg/g and that of BPP is 1.63 mg/g at initial concentration of 50 mg/L. The increase in adsorption capacity with increasing initial concentration is due to the fact that, at fixed adsorbent dose with increasing the metal concentration, all the available active sites of the adsorbent would be fully exposed to get occupied by the metal ions that are in excess saturating and yielding a higher adsorption capacity [47].

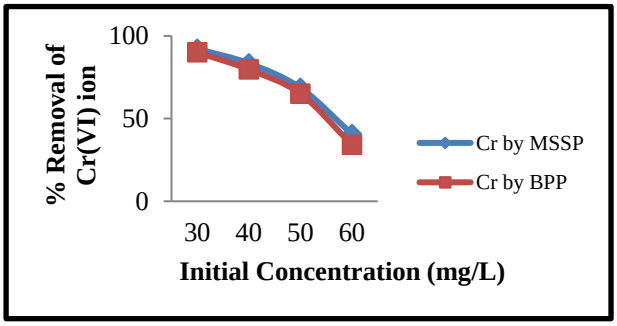

Figure 3.5. Effect of initial concentration on % removal of Cr (VI) by MSSP and by BPP. (dose 20 g/L, contact time 120 min. and pH 2 for Cr(VI) by MSSP and pH 4 for Cr(VI) by BPP)

3.6 Effect of Temperature

The effect of temperature on adsorption capacity of Cr(VI) onto MSSP and BPP was studied at a temperatures of 293 k, 313 k, 333 k and 353 k at the optimal conditions of the solution. As shown in Fig.3.6, an increase in temperature from 293 k to 353 k decreases the percentage removal from 91.40% to 37.93% that contains MSSP and from 90.03% to 33.80% for chromium solution that contains BPP respectively. Similar to percent removal, adsorption capacities of MSSP and BPP on the adsorption of Cr(VI) ion decreased from 1.37 mg/g to 0.57

mg/g and 1.35 mg/g to 0.51 mg/g with increasing temperature from 293 k to 353 k. This fall of metal uptake capacity of the adsorbents during the rise in temperature might be due to desorption caused by an increase in the available thermal energy. Higher temperature induces higher mobility of the adsorbate causing desorption or the damage of active binding sites in the biomass [48]. The decrease in adsorption capacity with increasing temperature indicates that adsorption process is exothermic in nature.

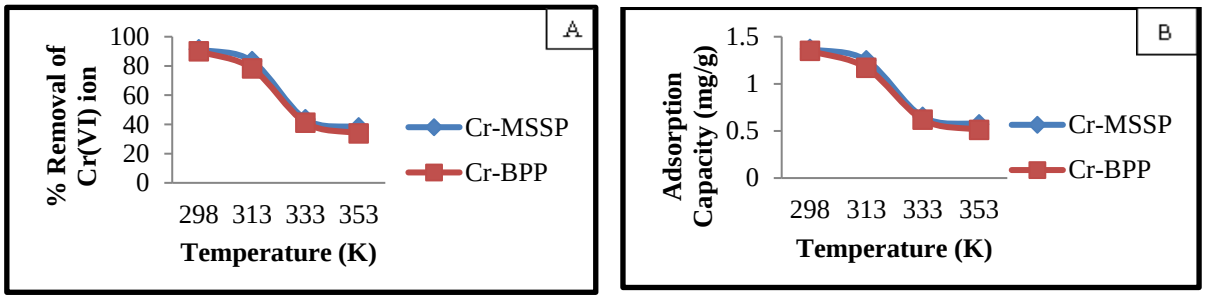

Figure 3.6. Effect of temperature on: a/ % removal of Cr(VI) and b/ adsorption capacity of MSSP (Concentration 30mg/L, dose 20 g/L, contact time 120 min. and pH 2 for Cr(VI) by MSSP and pH 4 for Cr(VI) by BPP).

3.7 Adsorption Isotherm

The Langmuir plot between $1/q_e$ vs $1/C_e$ for the sorption of Cr(VI) ion by MSSP and BPP are drawn in Fig. 3.7. It was found that the values of maximum adsorption capacity of MSSP and BPP were 9.709 mg/g and 7.353 mg/g, respectively (Table 1). The essential characteristics of the Langmuir isotherm can be explained by the equilibrium separation factor R_L. The R_L values for sorption of Cr(VI) ion by MSSP and BPP in this study were 0.325 and 0.275, respectively. This indicates that MSSP and BPP are favourable adsorbents for the removal of chromium

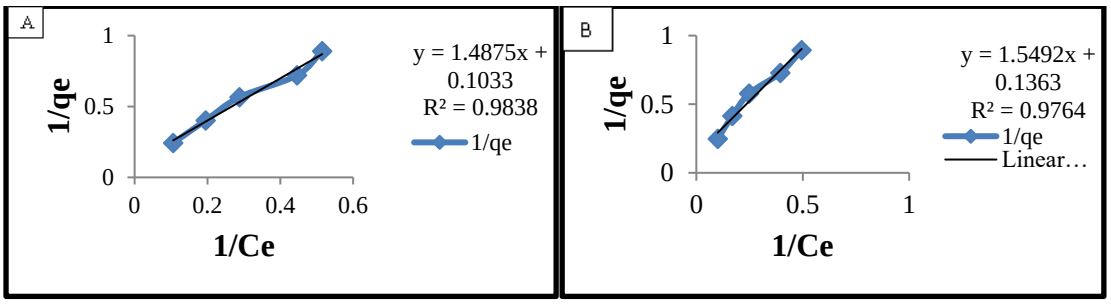

Figure3.7 Langmuir adsorption isotherms for: A/ Chromium by MSSP and B/ Chromium by BPP.

The Freundlich adsorption model is based on adsorption on heterogeneous surface and adsorption capacity related to the concentration of the adsorbent. The value of Freundlich constant 1/n and K_f for the sorption of Cr(VI) by MSSP and BPP were obtained from the slope

and intercept of the plot $\log q_e$ vs $\log C_e$. K_f which is an indicator of adsorption capacity of adsorbent and the higher the adsorption capacity, the higher the value of K_f. On the other hand, 1/n is a measure of intensity of adsorption. Therefore, the K_f value for the sorption of Cr(VI) ion by MSSP and BPP are 0.685 and 0.635 whereas the 1/n values for the sorption of Cr(VI) are 0.792 and 0.779 respectively. This indicates that both MSSP and BPP have high chromium sorption capacity and are favourable adsorbents from wastewater. The values of correlation coefficients (R^2) of the Freundlich model given in Fig.3.8, which were 0.993 and 0.983 for MSSP and BPP respectively and these values are larger than the R^2 values of the Langmuir model (0.983 and 0.976). This indicates the Freundlich model fits better to the adsorption data and thus it is more suitable to be used to describe the relationship between the amounts of Cr(IV) ion adsorbed by MSSP and BPP.

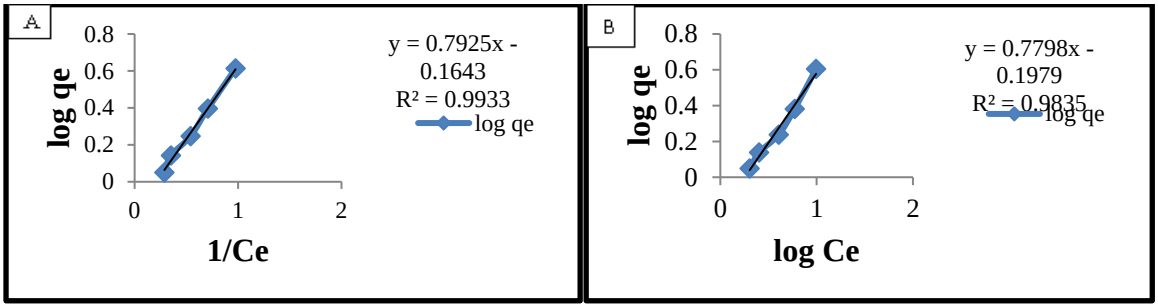

Figure 3.8 Freundlich adsorption isotherms for: A/ Chromium by MSSP and B/ Chromium by BPP

Table 1. Parameters of Langmuir and Freundlich adsorption isotherms of chromium

Metal ion	Langmuir isotherm				Freundlich isotherm		
	q_m	b	R_L	R^2	K_f	1/n	R^2
Cr(VI)-MSSP	9.709	0.0692	0.325	0.983	0.685	0.792	0.993
Cr(VI)-BPP	7.353	0.0879	0.275	0.976	0.635	0.779	0.983

3.8 Adsorption Kinetics

From the experimental data shown in Table 2, the calculated and experimental equilibrium adsorption capacity, q_e(cal) & q_e(exp), of pseudo-second-order kinetic model was close to each other than the pseudo-first-order kinetic model. This indicates that the pseudo-second order kinetics is the best kinetic model that fits to the experimental data for sorption of Cr(VI) by MSSP and BPP. The correlation coefficients (R^2) of pseudo-second-order kinetic model of chromium by MSSP and BPP (0.998 & 0.994) are closer to unity compared to the pseudo-first-order kinetic model (0.939&0.897). This indicates pseudo-second-order kinetic model is better model to the kinetics of adsorption onto the adsorbents it is indicated in Fig.3.9 and 3.10.

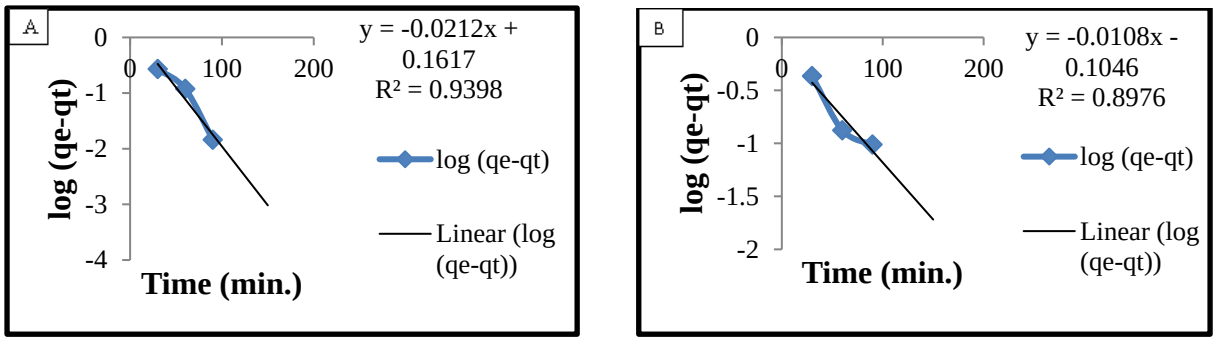

Figure 3.9 Pseudo-first order kinetics plot for A/ chromium by MSSP and B/ chromium by BPP

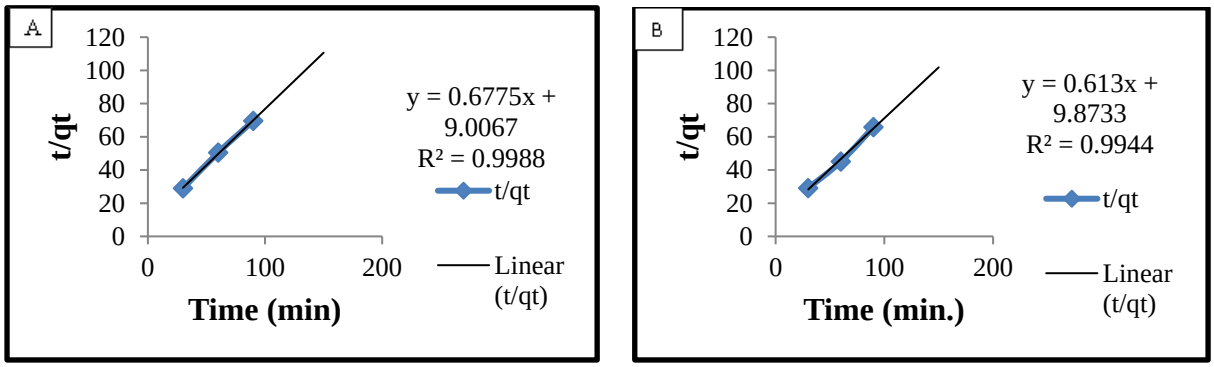

Figure 3.10 Pseudo-second order kinetics plot for A/ chromium by MSSP and B/ chromium by BPP

Table 2 Pseudo-first and second order constants for chromium by MSSP & BPP

		Pseudo first order kinetic model			Pseudo second order kinetic model		
Metal ion	q_{exp}	q_{cal} (mg/g)	k_1 (min^{-1})	R^2	q_{cal}(mg/g)	k_2 (g/mgmin)	R^2
Cr-MSSP	1.308	1.449	0.0484	0.939	1.477	0.051	0.998
Cr-BPP	1.4645	0.7870	0.023	0.897	1.631	0.038	0.994

3.9 Thermodynamics Study

The values of the thermodynamic parameters for adsorption of Cr(VI) ion onto MSSP and BPP are shown in Table 3. The increase in temperature made the values of ΔG^0 more positive. A negative value of Gibbs free energy change (ΔG^0) confirms the feasibility of the process and spontaneous nature of the sorption of Cr(VI) ion onto MSSP and BPP. The change in Gibbs free energy decreases with increasing temperature which indicates that a lower temperature favours adsorption.

The adsorption process involves energy changes that could result in a positive or negative value of ΔH^0. The negative values of ΔH^0 in this study indicates adsorption of Cr(VI) ion onto MSSP and BPP is exothermic in nature. If enthalpy change, (ΔH^0) of an adsorbent is higher than 40 kJ mol^{-1}, the process is said to be chemisorption which includes strong electrostatic chemical bonding between the metal ions and adsorbent surface. On the other hand, enthalpy change less than 20 kJ mol^{-1}indicate the physical nature of the adsorption process. In this study, all the values of ΔH^0 are greater than 40 kJ mol^{-1} revealing that chemisorption was responsible for the adsorption Cr(VI) ion onto MSSP and BPP. The positive values of entropy, (ΔS^0), indicate the increase in randomness of sorption processes of Cr(VI) ion at the solid-liquid interface of MSSP and BPP.

Table3 Thermodynamicparameters for Cr(VI)ionadsorptionontoMSSPand BPP atdifferent temperatures.

T (K)	Cr-MSSP				Cr-BPP			
	K_c	ΔG^o (kJ/mol)	ΔH^0 (kJ/mol)	ΔS^0 (kJ mol^{-1})	K_c	ΔG^o (kJ/mol)	ΔH^0 (kJ/mol)	ΔS^0 (kJ mol^{-1})
293	1.88	-1.535	39.28	0.129	2.21	-1.924	42.56	0.140
313	4.02	-3.617			5.57	-4.476		
333	26.05	-9.026			28.45	-9.275		
353	32.67	-10.243			38.94	-10.742		

4. Conclusions

From the current study, it can be concluded that the seed powders of *Moringa stenopetala* and banana peels can be used to remove Cr(VI) ion from wastewater. FT-IR characterization of the adsorbents showed that there was a change in the functional groups on the structure of both adsorbents before and after the adsorption processes. Percentage removal of Cr(VI) ion increases with decreasing pH, increasing adsorbent dose and contact time. Adsorption isotherm were described using the Langmuir and Freundlich models. The Freundlich model fits better to the adsorption data. The kinetics study reveals that the sorption of Cr(VI) ions are faster in the pseudo-second order kinetics than pseudo first order kinetics. Thermodynamic study was investigated using ΔG^0, ΔH^0 and ΔS^0 and the negative values of ΔG^0 shows the spontaneous nature of the sorption process and the positive value s of ΔS^0 indicates the randomness of the adsorption processes. The use of the greener bio-sorption process using MSSP and BPP adsorbents is important for the removal of Cr(VI) ions from wastewater in order yo safe the

environment. When comparing the two adsorbents, the removal efficiency of MSSP is better than BPP.

Abbreviations

MSSP – Moringa stenopetala seed powder

BPP – Banana peel powder

FT-IR – Fourier transformer infrared

ΔG^o – Gibbs free energy

ΔH – Enthalpy chang

ΔS – Entropy change

K – Equilibrium constant

k – rate constant

q_e – The amount of ions adsorbed (mg/g)

Q_m – the amount of ion adsorbed on monolayer (mg/g)

C_0 – Initial concentration of the ion (mg/L)

C_e – Concentration of ion at equilibrium (mg/L)

R – Universal gas constant (8.314 JK^{-1} mol^{-1})

Acknowledgements

The Authors would like to thank Arba Minch University Department of Chemistry for allowing us to use the laboratory facilities and resources during this research work.

Funding

This project has no any funding source.

Authors' contributions

TSB, AMY served as writer and editor of this manuscript and supervisor of the project.

EW served as producing the laboratory data and writing the manuscript. The author(s) read and approved the final manuscript

Authors Detail

Department of chemistry, College of natural and computational Sciences, Arba Minch University, Ethiopia

Availability of data and materials

The authors declare that the manuscript contains the minimal dataset that is required to interpret, replicate, and build upon the methods and findings reported in the article. Raw data can be shared via correspondence upon

reasonable request.

Ethics approval and consent to participate

Not applicable.

Consent for publication

Not applicable.

Competing interests

The authors declare that we have no competing interests

References

1. Hertel, R.F. (1986). Sources of exposure and biological e!ects of chromium. IARC Sci. Publ. 71, 63-77.
2. US Environmental Protection Agency (1984). Health effects assessment for hexavalent chromium. Prepared by the Office of Health and Environmental Assessment, Environmental Criteria, EPA/540/1-86-019, updated 1998.
3. Anderson, R.A. (1981). Nutritional role of chromium. Sci. Total Environ. 17, 13–29.
4. OSHA. (2006). Fact Sheet Health Effects of Hexavalent Chromium Hexavalent; OSHA: Washington, DC, USA
5. Saha, R., Nandi, R., Saha, B. (2011). Sources and toxicity of hexavalent chromium. J. Coord. Chem. 64, 1782–1806
6. Megharaj, M., Avudainayagam, S., Naidu, R. (2003). Toxicity of hexavalent chromium and its reduction by bacteria isolated from soil contaminated with tannery waste. Curr. Microbiol. 47, 51–54
7. Kleber, R.J., Helz, G.R. (1992). Indirect Photoreduction of Aqueous Chromium (VI). Environ. Sci. Technol. 26, 307–312.
8. Inamuddin, Yahya, A., Ismail. (2010). Synthesis and characterization of electrically conducting poly-o-methoxyaniline Zr(1V) molybdate Cd(II) selective composite cation-exchanger. Desal. 250, 523–529.
9. Ali, M., Inamuddin, Sardar, H. (2014). Poly (3,4-ethylenedioxythiophene): polystyrene sulfonate (PEDOT:PSS) Zr(IV) phosphate composite cation exchanger : sol-gel synthesis and physicochemical characterization. Ionics. 21, 1063–1071.
10. Milad, Sh., Mashallah, R., | Mohammad, Y. (2020). Producing water from saline streams using membrane distillation: Modeling and optimization using CFD and design expert. Int J Energy Res. 44 (11), 8841-8853.

11. Mahdi, Sh., et al. (2019). Application of ZnO nanostructures in ceramic and polymeric membranes for water and wastewater technologies. Chemical engineering journal. 391, 123475.
12. Marzieh, S. et al. (2019). Zeolitic imidazolate framework membranes for gas and water purification. Environmental Chemistry Letters. 18, 1-52.
13. Tolera, B., Vladimir, Sh. (2016). The electrodialysis of electrolyte solutions of multi-charged cations. 498, 86- 93.
14. Holan, Z.R., Volesky, B. (1995). Biosorption of heavy metals: Review *Biotechnology Progress*, 11, 235–250.
15. Ahluwalia, S.S., Goyal, D. (2007). Microbial and plant derived biomass for removal of heavy metals from wastewater. Bioresource Technology. 98, 2243–2257.
16. Sobhanardakani, S., Parvizimosaed, H., Olyaie, E. (2013). Heavy metals removal from wastewaters using organic solid waste rice husk, Environmental Science and Pollution Research. 5265–5271.
17. Jahn, S. A. A. (1991). The traditional domestication of a multipurpose tree Moringa stenopetala (Bak. F.) Cuf. In the Ethiopian Rift Valley, Ambio. 20: 244-247.
18. ICRAF. (2006). Moringa stenopetala", Avalable at http://www.World agroforestry.org/Sea/Products/AFD bases/AF/asp/Species Info.asp. (Accessed 8 September 2006
19. Demeulenaere, E. (2001). Moringa stenopetala, a subsistence resource in the Konso district. Proceedings of the International Workshop Development Potential for Moringa Products, October 29-November 2, 2001, Dar-Es-Salaam, Tanzania. 2-29.
20. Abuye, C., Urga, K., Knapp, H., Selmar, D., Omwega, A. M. and Imungi, J. K. (2003). A compositional study of Moringa stenopetala leaves, East African Medical Journal. 80, 247-252.
21. Jose, T.A., Silverio, B.S., Vasconcelos, L.M., Cavada, B.S. and Moriera, R.A. (1999). Compositional and nutritional attributes of seeds from the multipurpose tree Moringa oleifera Lam. J. Sci. Food Agric. 79, 815-820.
22. Food and Agriculture Organization Statistical Database. (2016). Available at http:// faostat 3. fao.org/download/T/*/E. Accessed June 23, 2016.
23. Food and Agriculture Organization Statistical Database. (2012). "Overview of World Banana Production and trade". The world banana economy, 1985-2012. Food and Agriculture Organization of the United Nations Corporate Document Repository.

Produced by Economic and Social Development Department, Rome, Italy. Available at http://faostat3.fao.org/home/index.html. Accessed June1, 2016.

24. Beed, F., Duboic, T., Markham, R. (2012). A strategy for banana research and development in Africa. A synthesis of results from the conference banana 2008, held in October 2008, Mombasa, Kenya. International Society for Horticultural Science, Belgium.
25. Foo, K.Y., Hameed, B.H. (2010). Insights into the modeling of adsorption isotherm systems. Chemical Engineering Journal. 156: 2-10.
26. Mohapatra, D., Mishra, S., Sutar, N. (2010). Banana and its by-product utilisation: An overview, AN Overv, Journal of Science and Industrial Research. 69: 323–329.
27. APHA Standard Methods for the Examination of Water and Wastewater 20th edition. (1998). Method 3500-Cr (D)-Colorimetric Method.
28. American Society for Testing and Materials. (1991). Standard Method for Moisture in Activated Carbon ASTM D 2867-91, Philadelphia, PA: ASTM Committee on Standards.
29. Dawodu, F.A., Akpomie, K.G. (2014). Simultaneous adsorption of Ni(II) and Mn(II) ions from aqueous solution onto a Nigeria kaolinite clay. Journal of Materials Research and Technology. 3. 129-141.
30. Deng, H., Yang, L., Tao, G., Dai, J. (2009). Preparation and characterization of activated carbon from cotton stalk by microwave assisted chemical activation. Application in mathylene blue adsorption from aqueous solution. Journal of Hazardous Materials. 166, 1514-1521.
31. Mahmood, T., et al. (2011). Comparison of different methods for the point of zero charge determination of NiO, Industrial and Engineering Chemistry Research. 50, 10017.
32. Lagergren, S. (1898). Zurtheorie der sogenannten adsorption gelosterstoffe. KungligaSvenskaVetenskapsakademiens. Handlingar. 24, 1-39.
33. Ho, Y.S., McKay, G., Wase, D., Foster, C.F. (2000). Study of the sorption of divalent metal ions on to peat. Adsorption Science and Technology.18, 639-650.
34. Langmuir, I. (1916). The constitution and fundamental properties of solids and liquids. Journal of American Chemical Society. 38, 2221–2295.

35. Thamilarasu, P., Sivakumar, P., Karanakaran, K. (2011). Removal of Ni(II) from aqueous solution by adsorption onto cajanuscajanL milsp seed shell of activated carbon. Journal of chemical Technology. 18, 414-420.
36. Thilagavathy, P., Santhi, T. (2013). Sorption of toxic Cr(III) from aqueous solutions by using treated Acacia nilotica leaf as adsorbent: single and binary system. Journal of Bioresources. 8, 1813–1830.
37. Kumar, M., Tamilarasan, R. (2013). Modeling of experimental data for the adsorption of methyl orange from aqueous solution using a low cost activated carbon prepared from Prosopisjuliflora. Journal of Chemical Technology. 15, 29-39.
38. Freundlich, H.M.F. (1906). Over the adsorption in solution. Journal of Physical Chemistry. 57, 385–470.
39. Meena, A.K., et al. (2005). Removal of heavy metal ions from aqueous solutions using carbon aerogel as an adsorbent. Journal of Hazardous Materials. 122, 161-170.
40. Padaki, S. R., et al. Kinetic studies on adsorption of chromium by coconut shell carbons from synthetic effluents, J. Environ. Sci. Health**.** 27, 2227-2241**.**
41. Attia, A. A., Khedr, S. A., Elkholy S. A. (2010). Adsorption of chromium ion (vi) by acid activated carbon. Brazilian Journal of Chemical Engineering. 27, 183 - 193.
42. Bhutada, P.R., et al.. (2016). Solvent assisted extraction of oil from Moringa oleifera Lam. seeds. Industrial Crops and Products. 82, 74–80.
43. Araújo, C.S.T., et al. (2010). Characterization and use of Moringaoleifera seeds as biosorbent for removing metal ions from aqueous effluents. Water Science and Technology. 62, 2198–2203.
44. Bhatti, I., Qureshi, K., Kazi, R.A. and Ansari, A.K. (2007). Preparation and characterization of chemically activated almond shells by optimization of adsorption parameters for removal of chromium (VI) from aqueous solutions. International Journal of Chemical and Molecular Engineering. 1(10), 105-110
45. Hammaini, A., et al. (2007). Biosorption of heavy metals by activated sludge and their desorption characteristics. Journal *of Environmental Management.* 84(4)**,** 419-426.
46. Özbay, N., Yargiç, R.Z., Yarbay, S., Önal, E. (2013). Full factorial experimental design analysis of reactive dye removal by carbon adsorption. Journal of Chemistry. 113. 4

47. Timbo, C.C., Kandawa-Schulz, M., Kwaambwa, H.M. (2017). Adsorptive removal from aqueous solution of Cr(VI) by green moringa tea leaves biomass. Journal of Encapsulation and Adsorption Sciences. 7, 108-119.
48. Donmez, D., Aksu, Z. (2002). Removal of chromium (VI) from saline wastewaters by Dunaliella species. Process Biochemistry. 38**:**751-762.